



Analytical and Experimental Investigation of I Beam-to-CFT Column Connections under Monotonic Loading

G. R. Abdollahzadeh*, S. Yapang Gharavi, M. Hoseinali Beigy

Department of civil engineering, Babol University of Technology, Babol, Iran

PAPER INFO

Paper history:

Received 29 July 2013

Received in revised form 23 August 2013

Accepted 14 September 2013

Keywords:

Endplate Connection

CFT Column

Moment-rotation Curve

I Beam-to-CFT Column Connection

ABSTRACT

In this study, the behavior characteristics of I beam-to-concrete filled tube (CFT) column connection is studied through experiment and finite element models under the monotonic loading. To validate the finite element modeling, at first, an experimental model is made and experimented. After validation of the finite element modeling, different models were created in the software. The studied parameters include the endplate thickness and the connection type. Various types of endplate thickness are studied for bolted and weld connections. For bolted connections, different types of I beam-to-CFT column connections are studied using the bolts passing and not passing through the CFT section. The results show that increase in endplate thickness leads to increase in the connection flexural strength and stiffness and decrease in rotation in a specific resistance value.

doi: 10.5829/idosi.ije.2014.27.02b.13

1. INTRODUCTION

Buildings with composite steel-concrete framing are increasing around the world, as they combine the advantages of the high erection speed and the ductility of the steel structures as well as, the high compressive strength of the concrete. The concrete-filled steel tube column is advantageous since the steel tube provides confinement. Thus, it increases the stiffness and strength of the concrete, while the concrete reduces the possibility of the local and global buckling of the tube wall. Moreover, the steel tube column eliminates the column formwork during construction.

A wide range of beam-to-CFT column connections have been studied over the past several decades. A convenient connection is attaching the steel beam directly to the skin of the steel tube for simple connections [1, 2]. However, Alostaz and Schneider [3, 4] have shown that welding the beam directly to the steel tube should not be used in moment-resisting frames. Severe tube wall distortions can prohibit the development of the plastic bending capacity of the beam, and cause very large stresses and strains on the flange weld and the tube wall. In contrast, bolted

connections or combinations of “field bolted-shop welded” connections have better performance [5], as they don’t deal with problems related to the brittle weld failure observed in the 1994 Northridge and 1995 Kobe earthquakes [6, 7]. In moment end-plate (MEP) connections, all welding can be performed in the factory, where it is possible to obtain higher quality control, rather than in the field, where the welding can be time consuming and costly. MEP connections are easy to erect and cost approximately the same as other moment connections.

Prion and McLellan [8] proposed a connection, consisting of beam end-plates attached to the CFT column using through-column bolts which showed good behavior. Chung et al. [9] and Wu et al. [10, 11] also demonstrated that good performance is possible but it requires appropriate design and detailing of the bolted connections. Chung et al. [9] and Wu et al. [10] also tested the bolted beam to rectangular CFT column connections with stiffened extended end-plates.

Structural joints exhibit a distinctively nonlinear behaviour that results from a multitude of phenomena including elastoplastic deformations, contact, slip and separation of their elemental parts. The joint behavioural characteristics can be represented by means of a moment-rotation ($M - \phi$) curve that defines three main properties: resistance, stiffness and rotation

*Corresponding Author Email: abdollahzadeh@nit.ac.ir (G. R. Abdollahzadeh)

capacity. Historically, moment resisting joints have been designed for resistance and stiffness with little regard to rotational capacity. Yet, the knowledge of the available rotation capacity of structural joints is of utmost importance for designing partial strength joints in combination with a plastic global analysis or under seismic conditions. The present study aims at describing the bolt connection of I beam to CFT column using the endplate (Figure 1) and also the weld connection of I beam-to-CFT column. It must be mentioned that for some samples, the bolts passing through the CFT section, are used to provide continuity between the column flanges. Proper models for CFT columns subjected to an axial compressive force and bending moment in combination are proposed. The models verified by using the nonlinear finite element program ABAQUS compared against experimental data by Hsuan-Teh Hu et al. [12]. Various experimental and analytical studies have been performed on CFT columns [13-15]. The concrete core adds stiffness and compressive strength to the tubular column and reduces the potential for inward local buckling. On the other hand, the steel tube acts as longitudinal and lateral reinforcement for the concrete core helping it to resist tension, bending moment, shear, and preventing the concrete from spalling. Past studies -Furlong, Knowles and Park, Boyd et al., Roeder et al., Neves et al. [13-17] have shown that due to the benefit of composite action of the two materials, the CFT columns provide excellent structural properties such as high strength, high ductility and high energy absorption capacity. In the present study, I beam-to-CFT column connection under monotonic loading is experimented for the bolted connection (Figure 1), and afterwards, the finite element model of this experimental specimen is prepared. Validity of the performed modeling is ensured by comparing the experimental and analytical results. Therefore, subsequent various models are made similarly for both bolted and welded connections in order to validate the connection evaluation through using more data.

2. EXPERIMENTAL PROGRAM DESCRIPTION

2. 1. The Experimental Details The experimental sample is basically made of I beam, CFT column, concrete and the endplate. The endplates are connected to the beam by 45° full-strength welds. The manually tightened 8.8 M20 bolt type with 22-millimeter-diameter holes are used in the experiment. The concrete with low-strength of 15 MPa is used to fill the hollow section. The geometric design of the experimental sample and the related details are illustrated in Figure 2 and Table 1.

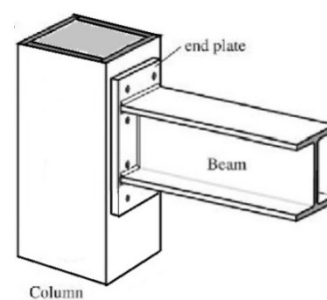


Figure 1. I beam-to-CFT column connection with endplate

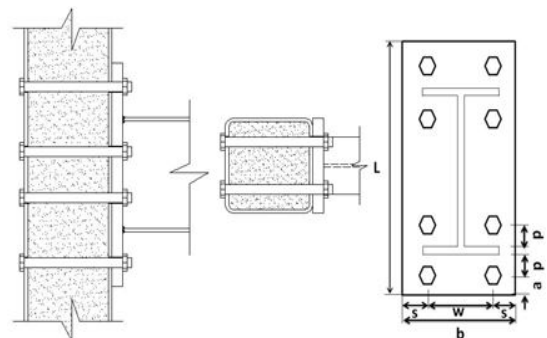


Figure 2. Geometric properties of specimens

TABLE 1. Details and geometric properties of experimental specimen

Beam (mm)	Column (mm)	Endplate (mm)						
		L	b	t	w	s	a	p
IPE 240	Box 200x200x8	470	200	25	100	50	50	65

TABLE 2. Average characteristic values for the structural steels and bolts

Specimen	f_y (Mpa)	f_u (Mpa)	E (Gpa)	ρ_y
Beam IPE 240	324.03	431.2	201.6	0.75
Column Box 200x200x8	337.3	446.5	204.86	0.755
Endplate	353.4	485.23	201.25	0.728
Bolts	633	896	209	0.64

2. 2. Tension Test of the Structural Steel and Bolts

Materials for the tensile test coupons are cut from the flanges and webs of the steel beams, square tube and endplate. Values of the yield strength and ultimate strength of the steel members are obtained by testing one strip coupon of each member. The tensile test of the structural steel and bolts are performed in the laboratory. Results are listed in Table 2. The listed values include the yield stress (f_y), the ultimate stress (f_u), the Young modulus (E) and the yield ratio $\rho_y = f_y / f_u$. Gioncu and Mazzolani [18] have stated that a proper deformation is assured when $0.5 \leq \rho_y \leq 0.7$ and the full-strength steels with $\rho_y > 0.9$ imply a relative weak deformation. According to the Eurocode3 [19], a proper deformation is assured when $\rho_y > 0.83$. The assurance of a suitable material ductility does not necessarily imply that the whole structure is ductile. The structural ductility depends on the yield ratio but especially on the structural discontinuities, such as welds, bolt holes and other types of connections.

2. 3. The Experiments Equipment

The experimental equipment and their locations are shown in Figures 3. Loading is performed by the experiment device Enerpac, ZE5 model, which is connected to the load measurement device (loadcell) with 1MN capacity. Loadcell, from its free end, is connected to the beam by the specified device. Linear transducers (LVDT) with strokes ranging from 25 mm to 100 mm placed on the beam and on the column are used to measure the displacements as shown in Figure 4. In Figure 4, LVDT no. 4 measures the displacement of the beam at mid-span. LVDT no. 5 enable the evaluation the rotation of the beam in the section close to the joint, that is, the rotation of the joint plus the column rotation (as a whole and by shear at the joint). All these measurements give redundant evaluations of the beam rotation. The column rotation is measured by LVDTs. 7 and no. 8 to evaluate the rigid body rotation. The load value, the vertical displacement of the beam, the horizontal displacement of the endplate and the column in desired points are measured by the related measuring equipment. The test control and the data acquisition system are run by a Windows-based control and acquisition program.

2. 4. Setup and Experiment Process

Before mounting specimens on the experimental frame, dimensions are measured and recorded and bolts are tightened. Then, specimens are installed and aligned in the frame. The boundary conditions of the experimental samples are prepared in such a way that the behaviour of experimental samples are as close as possible to their real behavior. The samples can be colored with the plaster water or the limewater in order to characterize the pattern of yield lines. Next step is the measurement equipment installation. All the measurement equipment

is connected to the recording device with the extension cords. Afterwards, samples are exposed to the monotonic compression or tension which depends on the location of the loading device. To figure out the sample behavior, it is important to observe and record the apparent deformations of the samples including the plastic deformations and specifically the position of the plastic hinge, local and overall buckling of components, and finally the probable rupture and disconnection of sample components and welds. There are different methods to observe the plastic deformations in parts of samples. One of these methods is to cover the sample with a thin coating of the limewater. Therefore, before the test, faces of the samples are covered with the limewater. The dried lime is very fragile and will crack due to the relative deformations of the steel above the yield limit. These cracks indicate that which parts have reached the yield limit. Moment-rotation and force-displacement curves and other required information are ultimately obtained through using the derived data.



(a)



(b)



(c)

Figure 3. (a) Equipment and test specimen, (b) details of connection zone, (c) details of the load device

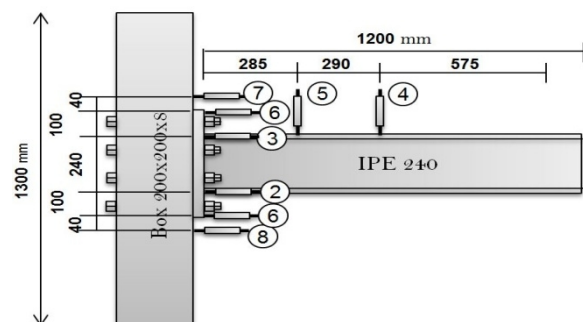


Figure 4. Location of the displacement transducers.

3. THE FINITE ELEMENT MODELING

3. 1. Experiment Results and the Finite Element Model of the Experimental Specimen

3. 1. 1. Generalities To verify the results of the finite element modeling, the experimental specimen is made and tested. The ABAQUS finite element software is used to model the bolted endplate connection. In modeling of different parts such as concrete and steel, the studies of Hsuan et al. [12] have been used. The modeling is performed regarding the following hypotheses:

- ❖ All the connection components including beam, column, endplate and bolts are modeled by the nodal element Solid Deformable. This element is capable of considering the plasticity process and the phenomena of the great rotations and strains.
- ❖ The holes of the bolts are modeled 2 mm bigger in diameter than the bolts.
- ❖ The friction coefficient of the contacting surfaces is supposed to be 0.6.
- ❖ To consider the interactional effects of the connection components, all the adjacent surfaces including the surfaces of the endplate and the column, beam and endplate, bolt and the column surface, bolt and the column hole, bolt and the endplate hole, bolt and spanner, spanner and the endplate, concrete surface and the inner surface of the column, bolts and the concrete, are mixed according to the interaction definition which is one of the capabilities of the ABAQUS software. Hence, during the loading steps, the penetration of the nodes of the adjacent surfaces is not possible. The contact elements Tangential behavior and Normal behavior are applied for this purpose.
- ❖ Non-linear properties are considered for all the materials of the connection components including bolts, spanners, endplate, beam and column. The stress-strain curves used for the steel and for the bolts are shown in Figure 5.
- ❖ In order to mesh the components, the regular meshing (element classification) is used. The element dimensions in different parts are proportional to the required accuracy. The stress changes are more in the connection zone than that in farther zones in the beam and the column. Therefore, finer meshing is used in the connection zone.
- ❖ The properties of all the materials of the model are supposed to be isotropic. The isotropic hardening rule is used for the plastic deformation of the steel.

The dimensions of the primary modeling are the same as those of the experimental sample so that the reliability of the obtained results can be evaluated.

The diagrams are drawn according to the applied loading and direct recording of the displacement,

bending moments and their consequent deformations. The bending moment (M) acting on the connection corresponds to the applied load; in other words, “Load” multiplied by the distance between the load application point and the face of the endplate, L_{load} :

$$M = Load \times L_{Load} \tag{1}$$

The rotational deformation of the connection (Φ) is the sum of the shear deformation of the column web panel zone (γ) and the connection rotational deformation, (ϕ). Connection rotation is defined as the change in angle between the centerline of beam and column (θ_b, θ_c) [20]:

$$\phi = \theta_b - \theta_c \tag{2}$$

In this test, the column deforms hardly. Then, both γ and θ_c are naught. Considering the LVDTs installed on the column, finally, rotations and displacements will be subtracted from θ_b or ϕ , or can be used to calculate θ_c . The beam rotation can be calculated according to the following equation:

$$\begin{aligned} \theta_b &= \arctan \frac{\delta_{DTi}}{L_{DTi}} - \theta_{b.el} = \arctan \frac{\delta_{DT4}}{575} - \theta_{b.el} \\ &= \arctan \frac{\delta_{DT5}}{285} - \theta_{b.el} \end{aligned} \tag{3}$$

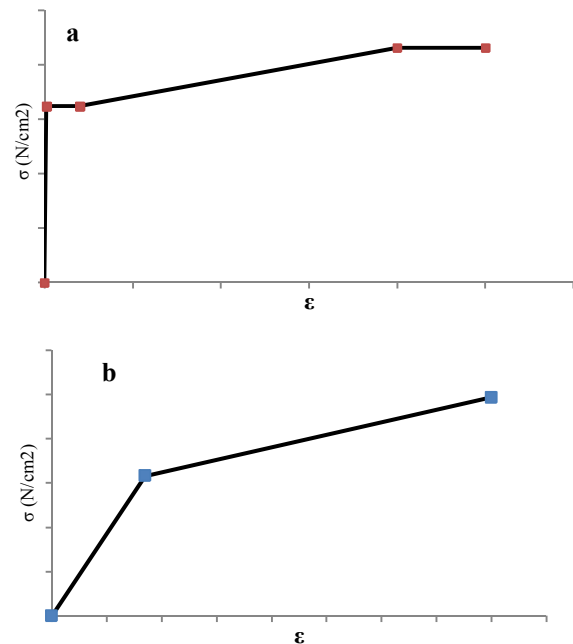


Figure 5. (a) The stress-strain curve for the steel, (b) The stress-strain curve for the bolt

where, δ_{DTi} are the vertical displacement at LVDT DTi and $\theta_{b,el}$ is the beam elastic rotation. $\theta_{b,el}$ can be calculated by the equation: $\theta_{b,el} = \frac{FL_F^2}{2E_b I_b}$,

where, F is the applied load, L_F is the distance between the load application point and the face of the connection, E_b is the young modulus of the beam, and I_b is the second moment of the beam [21, 22].

The effects of shear deformation in the beam are ignored in above discussions and it is assumed that the vertical displacement of the endplate is insignificant. The $(M - \phi)$ curve of the connection can be drawn according to the above information. The main properties of this curve include strength, stiffness, and the rotational capacity.

3. 1. 2. Moment-Rotation Curves As mentioned above, $(M - \phi)$ curves of different connections are derived from recording the vertical displacement of the beam and the amount of the applied load. The Figure 6 shows the amount of the applied load against the vertical displacement of the beam. This curve can be converted into moment-“gross beam rotation” curve through application of Equations (1) and (3) excluding $\theta_{b,el}$, as shown in Figure 7(a) for LVDTs DT4 and DT5. Ana et al. [21] and Davor et al. [22] showed that as the distance between DTi and the connection decreases, its difference from other DTs will increase. The reason for the difference between DT4 and DT5 is the less distance between DT5 and the endplate. Hence, the results obtained from DT4 are used for more investigations. If the elastic deformation of the beam is subtracted from the gross rotation (Equation (3)), the connection rotation can be completely indicated (Figure 7(b)). Provided that the rotation of the θ_c column can be ignored compared to the θ_b column (Figure 8), the connection rotation value can be considered equal to the beam rotation. This happens because the endplate vertical deformation due to the bolt hole elongation can be neglected when compared to δ_{DT4} .

An experiment is performed in the laboratory under the monotonic loading for the endplate connection with 25 mm thickness. The results of this experiment are presented regarding the applied load, direct recording of the displacements, the applied bending moment and its subsequent deformations. Figure 8 shows the deformed ones.

The $(M - \phi)$ curve of the experimental connection and corresponding finite element model are shown in the Figure 10. In particular, the following characteristics are assessed for the test: knee-range of the $M - \phi$

curve, the plastic flexural resistance, ($M_{j,Rd}$), the maximum bending moment, (M_{max}), the initial stiffness, ($S_{j,ini}$), the post-limit stiffness, ($S_{j,p}$), the rotation corresponding to the maximum loading, ($\phi_{M_{max}}$) and the rotation capacity, (ϕ_{Cd}) [21, 22]. The ductility can be indicated with the index, ψ_j , that relates the maximum rotation of the connection, ϕ_{max} , to the rotation corresponding to the connection plastic resistance, $\phi_{M,Rd}$, which can be calculated from the Equation (5). Simões et al. [23] and Kuhlmann et al. [24] showed that the experimental value of the plastic resistance cannot be easily evaluated. Hence, two levels of resistance are considered: the lower and upper limits of the knee-range.

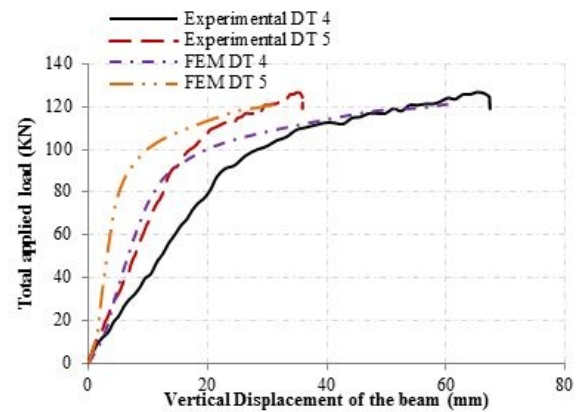
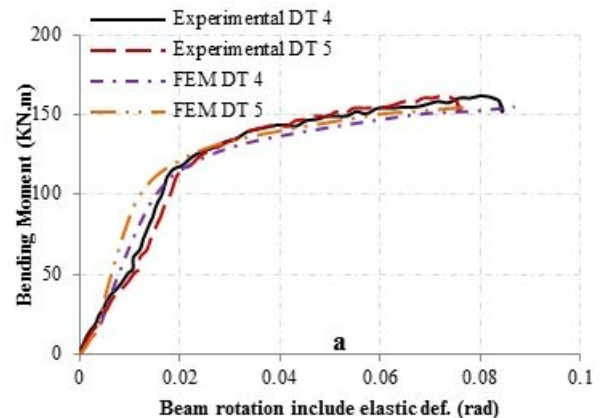


Figure 6. Beam vertical displacement readings of LVDTs DT4-5



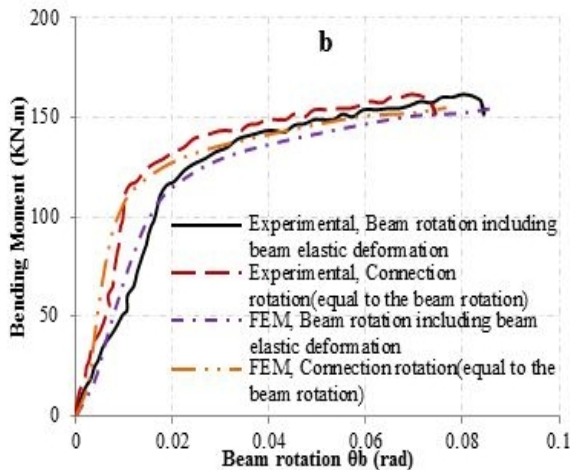


Figure 7. (a) Beam rotation computed from the displacement readings of LVDTs DT4 and DT5 ($\arctan(\delta_{DTi}/L_{DTi})$). (b) Beam rotation computed by means of Equation (4) from the displacement readings of LVDT DT1.

$$\psi_j = \frac{\phi_{max}}{\phi_{M,Rd}} \quad (4)$$

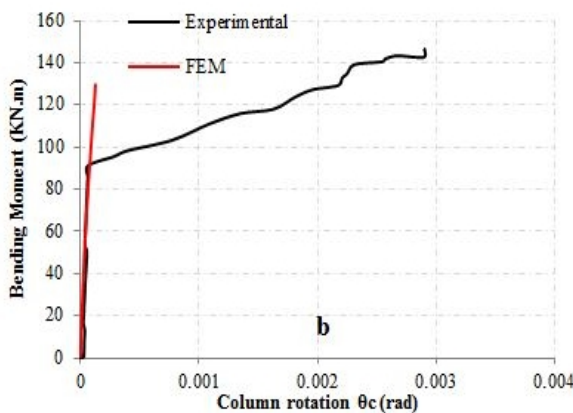
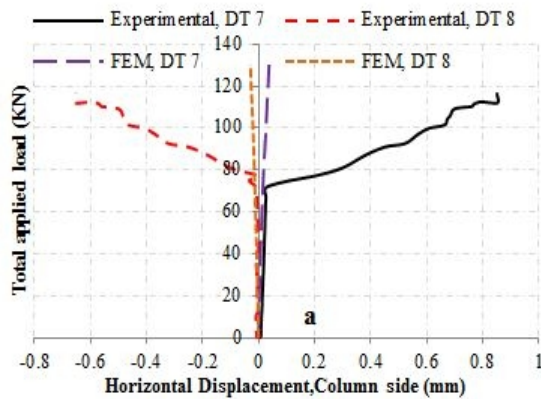


Figure 8. Connection rotation, (a) Column horizontal displacements, (b) Corresponding column rotations ($\theta_c = \arctan((|\delta_{DT7}| + |\delta_{DT8}|)/(h_{DT7-8}))$)

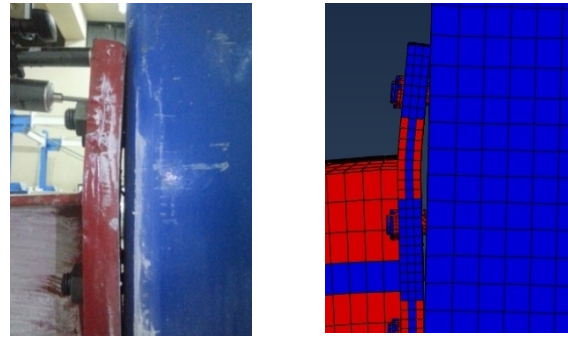


Figure 9. Deformed shape of the test specimen and finite element model

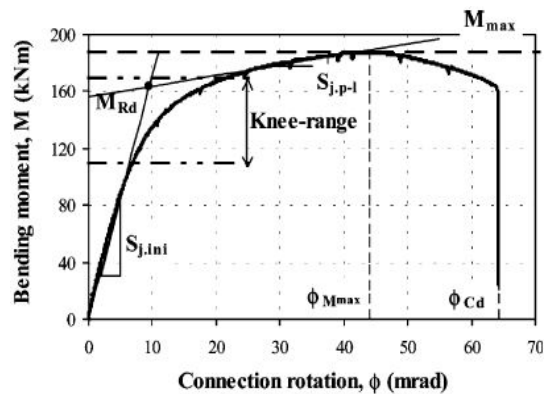


Figure 10. Moment-rotation characteristics from tests

In general, it can be said that the finite element model is reliable enough to predict $M - \phi$ curve. This model is also able to effectively estimate the initial stiffness and resistance and even the rotational capacity of the connections provided that the real nonlinear properties is considered for all of the materials of the connection including the bolts, endplate, beam and column. Comparing the finite element model and the experimental result shows higher stiffness and resistance and less rotation for the experimental result. This difference is significant especially for the initial stiffness. The main features of the moment-rotation curve of the experimental specimen and that of the finite element model are presented in Table 3. Table 4 represents the summary of statistical processing of the results. All of these values are derived from the recordings of LVDT DT4.

The relative error of the finite element model in calculating the initial stiffness, ultimate resistance and rotation are listed compared with the experimental values.

The real ($M - \phi$) curve can be satisfactorily predicted by the finite element model. A relative error of 12% for initial stiffness is obtained for the finite element model compared with the experimental one. The higher value of the initial stiffness in the finite

element model compared to that of the experimental results is due to the further fixity of the finite element model or more degrees of freedom in the experimental specimen. The finite element model is acceptable to predict the initial stiffness. There are differences between the results of the finite element model and that of the experimental one, perhaps, because a fairly advanced finite element modeling is very time-consuming and expensive and requires powerful computers. Therefore, in the current study, simpler finite element modeling is performed.

After comparing the ultimate resistance of the finite element and experimental model, a relative error of 2.7% is calculated. This shows that the finite element model was more successful in predicting the ultimate resistance.

And finally, after comparing the rotation of the finite element and experimental model, a relative error of 5% was calculated.

3. 1. 3. Behavior of the Tension Zone The most significant characteristic describing the overall deformation behavior in the tension zone is the force-displacement response or the moment-displacement response. The obtained information from LVDT DT 3 shows the deformation behavior of the endplate in the tension zone. For example, the Figure 11 presents the moment-displacement curves for the experimental specimen and the finite element model which were obtained from DT2 and DT3. According to this figure, the values obtained for the deformation and ultimate displacement of the endplate for the finite element model are acceptable compared with experimental results. The difference between the experimental results and the finite element model can be attributed to the following general reasons:

- ❖ Imperfections, lack of fit and residual stresses of the experimental setup (Bursi and Jaspert, Lemonis and Gantes) [25, 26], which cannot be easily considered in the finite element modeling. These factors can strongly affect the initial stiffness.

- ❖ Lack of accuracy of the displacement measuring devices.
- ❖ Not using a fairly advanced and accurate finite element modeling due to the need to powerful computers and knowing the related software well and its time-consuming nature.

According to the obtained results, the accuracy of the finite element model results can be considered acceptable. Therefore, the finite element modeling of other samples has been similar to the previous model.

3. 2. Properties of Various Presented Connections In this study, different types of I beam-to-CFT column connection are investigated. These types include:

1. The Bolted connection with creating continuity between the column flanges by bolts passed through the column section (BEP) with different thicknesses for the endplate.
2. The Welded endplate connection without continuity between the column flanges (WEP) with different thicknesses for the endplate.
3. The direct welded connection of I beam-to-CFT column, without continuity between the column flanges (W).

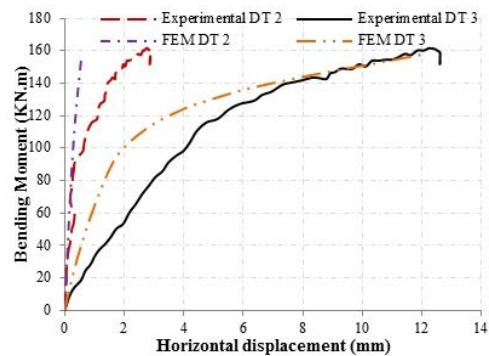


Figure 11. Moment-displacement curve of endplate for the experimental and the finite element model

TABLE 3. Main characteristics of the moment-rotation curves

	Resistance [KNm]		Stiffness [KNm/mrad]		Rotation [mrad]	
	$M_{j,Rd}$	M_{max}	$S_{j,ini}$	$S_{j,p}$	ϕ_{Mmax}	ϕ_{Cd}
Experimental	129.2	161.6	11.01	0.51	68.3	73.5
FEM	123.3	157.3	12.3	0.46	76.2	77.2

TABLE 4. Relative errors of experimental results and finite element model

Relative error	Resistance [KNm]		Stiffness [KNm/mrad]		Rotation [mrad]	
	$M_{j,Rd}$	M_{max}	$S_{j,ini}$	$S_{j,p}$	ϕ_{Mmax}	ϕ_{Cd}
	0.05	0.027	-0.12	0.1	-0.12	-0.05

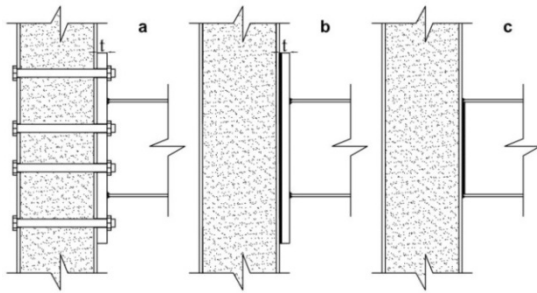


Figure 12. Types of connection

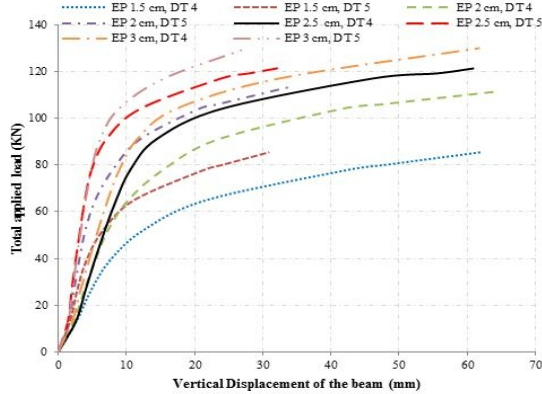


Figure 13. Beam vertical displacement for finite element models with BEP connection type

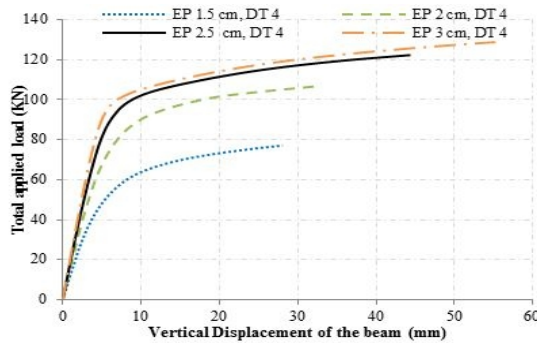


Figure 14. Beam vertical displacement for finite element models with WEP connection type

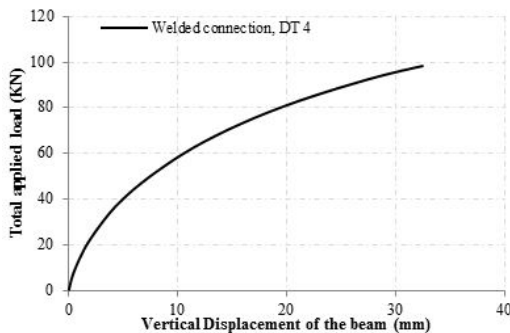


Figure 15. Beam vertical displacement for finite element model with W connection type

Connection specimens are shown in Figure 12. General properties of the connections are illustrated in Figure 2. Four different thicknesses of 15, 20, 25, and 30 mm for the endplate are modeled for the WEP and BEP connection types. In the previous sections, the results of the model with the 25mm thick endplate have been discussed and compared to the experimental results. Here, for all models, it is assumed that welds and bolts will never rupture.

3. 3. Evaluation of the Results of Various Finite Element Models In the previous sections, it is demonstrated that the finite element model is reliable to predict $M-\phi$ curves. This model is also able to effectively estimate the initial stiffness and resistance or even the rotational capacity of the connections providing that the real nonlinear properties is considered for all the materials of the connection including the bolts, endplate, beam and the column. The results of the finite element model and the experimental results are also discussed in previous sections. According to the results, accuracy of the finite element model can be considered acceptable. Thus, the finite element modeling of other samples is performed similar to the previous model.

The $(M-\phi)$ response of the connections is presented in Figures 13 to 15. As described before, $(M-\phi)$ curves of different connections are derived from recordings of the vertical displacement and the applied loading. The applied loading against the vertical displacement of beam, for different models is shown in Figures 13 to 15. The rotation of the beam for finite element models is calculated by recordings of LVDTs DT4 and DT5 displacement. The rotation of the beam for finite element models is calculated by the Equation (3), through recordings of LVDT DT4 displacement. These values are presented in Figures 16 to 18 in which BR is “Beam rotation including beam elastic deformation”, and CR is “Connection rotation (equal to the beam rotation)”.

In WEP and W connections, due to lack of realistic modeling of the nonlinear properties of materials and their yielding, the ultimate yield point and maximum strength is not detectable. Hence, the control strain is used to determine the yield point in present study. However, at this stage, the aim is to compare and evaluate the initial stiffness.

According to the Figure 8, the column rotation can be ignored. The column rotation is also disregarded in finite element models. The $(M-\phi)$ curve of the BEP, WEP and W connections of the finite element models are shown in Figures 19 to 21, respectively. The main features of the moment-rotation curve for the finite element models are presented in Table 5. All these values are derived from LVDT DT4.

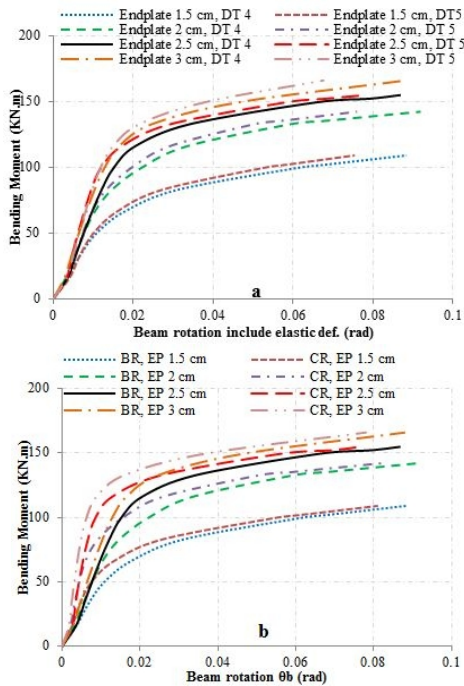


Figure 16. (a) Beam rotation for finite element models of BEP connections computed from the displacement readings of LVDTs DT 4-5 ($\arctan(\delta_{DTi}/L_{DTi})$), (b) Beam rotation for finite element models of BEP connections computed by means of Equation (4) from the displacement readings of LVDT DT4.

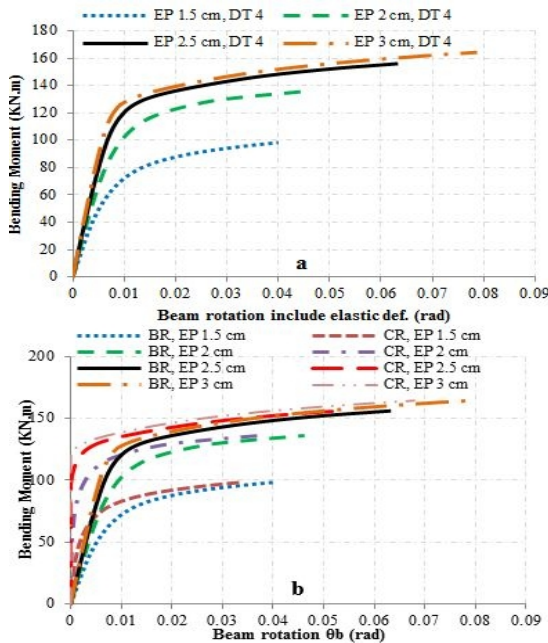


Figure 17. (a) Beam rotation for finite element models of WEP connections computed from the displacement readings of LVDT DT 4 ($\arctan(\delta_{DTi}/L_{DTi})$), (b) Beam rotation for finite element models of WEP connections computed by means of Equation (4) from the displacement readings of LVDT DT4.

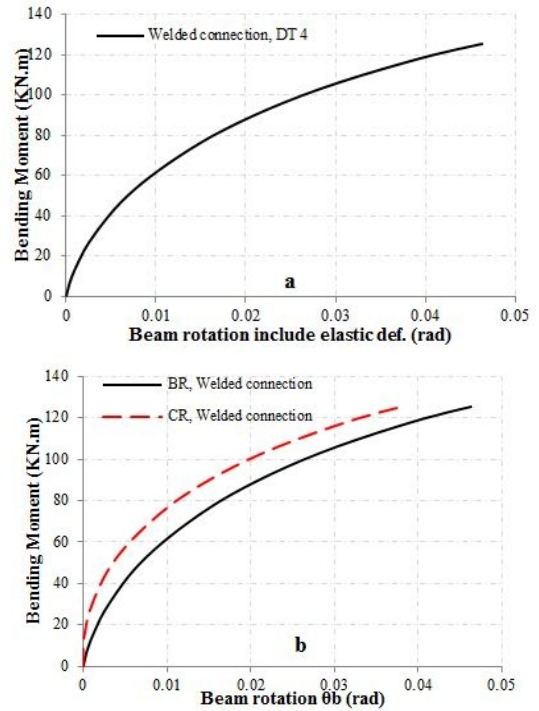


Figure 18. (a) Beam rotation for finite element model of W connection computed from the displacement readings.

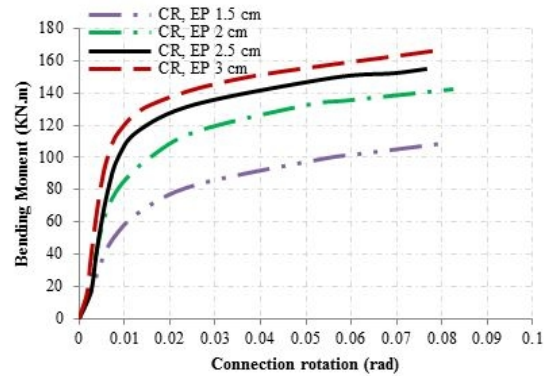


Figure 19. Moment-rotation curve of BEP connections

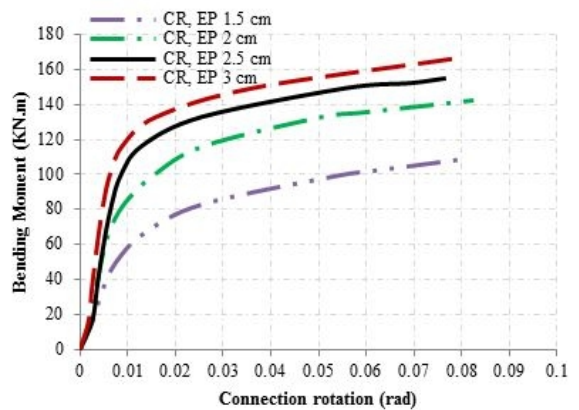


Figure 20. Moment-rotation curve of WEP connections

TABLE 5. The main features of moment-rotation curves

Connection Type	Resistance [KNm]		Stiffness [KNm/mrad]		Rotation [mrad]		
	$M_{j,Rd}$	M_{max}	$S_{j,ini}$	$S_{j,p}$	ϕ_{Mmax}	ϕ_{Cd}	
FEM, BEP	t = 15 mm	81.3	109.1	8.3	0.59	82	82
	t = 20 mm	108.4	142.28	11.2	0.6	81	81
	t = 25 mm	123.3	157.9	12.4	0.47	77.2	77.2
	t = 30 mm	136.7	165.4	14.7	0.46	77.3	77.3
FEM, WEP	t = 15 mm	-	98.62	42.99	-	33.53	33.53
	t = 20 mm	-	136.12	885.48	-	37.2	37.2
	t = 25 mm	-	156.04	Infinity	-	53	53
	t = 30 mm	-	164.34	Infinity	-	67.9	67.9
FEM, W	-	-	125.45	219.3	-	38.1	38.1

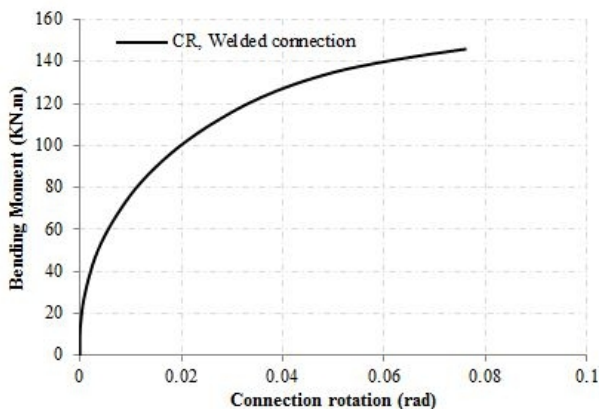


Figure 21. Moment-rotation curve of W connection

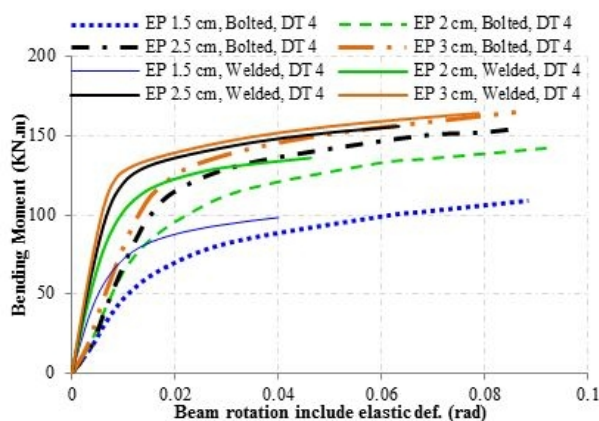


Figure 22. Moment-rotation curves for welded and bolted connections with endplate

According to Table 5 and Figure 19, the results of the BEP connections indicate that generally, the

increase in the thickness of the endplate leads to increase in the connection flexural resistance and stiffness and decrease in the rotation in a specific resistance value. The values ϕ_{Cd} and ϕ_{Mmax} are the same because the rupture is not considered in the modeling.

In WEP and W connections, due to lack of realistic modeling of the nonlinear properties of materials and their yield, the ultimate yield point and maximum strength is not detectable. In this study, the control strain is used to determine the yield point; But, from the curves of these types of connections, trend of change can be examined and at this stage, the aim is to compare and evaluate the initial stiffness. According to Figure 20, the results of the WEP connection show that generally, increase in the thickness of the endplate leads to the increase in the connection flexural resistance and stiffness and decrease in the rotation in a specific resistance value. In these types of connections, assuming no rupture in the welds, the initial stiffness increases by increase in the endplate thickness (see related diagrams and Table 5). Since ruptures are not considered in modeling, only the turned of changes are discussed.

In W connection, at first, the initial stiffness is infinite and then it decreased in the subsequent steps. The decreased value is reported in the Table 5.

Comparing the curves of welded and bolted connections in Figure 22 shows that welded connections have more rotational stiffness, less ultimate strength, less ultimate rotation and less ductility than that bolted connections do. Regarding the area under the curves, it can be said that bolted connections have more ductility and energy absorption capacity than that welded connections do.

In bolted connections, in most cases, the bolts and the endplate are considered as the main sources of deformation.

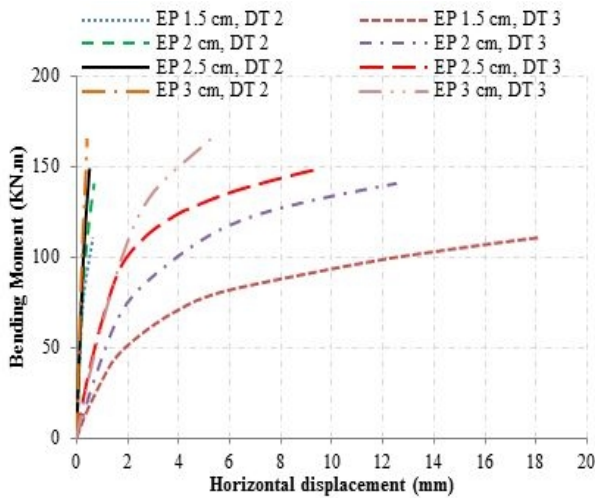


Figure 23. Endplate moment-displacement curve for the finite element model of BEP connection type

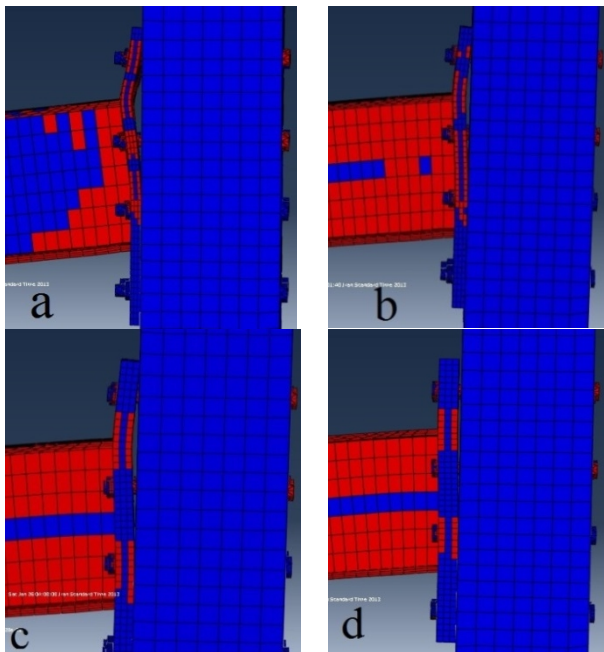


Figure 24. Deformation of the finite element models of BEP connections, (a) 15 mm, (b) 20 mm, (c) 25 mm, (d) 30 mm

As stated before, the most significant characteristic describing the overall deformation behavior in the tension zone is the force-displacement response or the moment-displacement response. Figure 23 shows that the endplate deformation decreases as its thickness increases. This behavior is expectedly similar to the connection rotation, because the components of the endplate and bolts are the main sources of connection deformation. Deformed shapes of the endplate in the BEP connections are shown in Figure 24.

5. CONCLUSION

A new steel and concrete composite moment resisting frame system was proposed along with innovative connection details.

For the bolted connections, an experiment was performed with the extended endplate of a specific thickness, under the monotonic loading. Afterwards, similar to the experimental specimen, 4 bolted endplate connections were modeled with different thicknesses as the finite element model. The finite element model for welded endplate connection with 4 various thicknesses and then a directly welded beam-to-column connection were made. From the experimental and analytical studies on the full-scale steel beam to CFT column connection models, the following conclusions can be drawn:

1. The proposed connection for the steel beam to the CFT column bolted composite connections exhibited good ductility and energy-dissipation capacity.
2. The experimental model had an inelastic rotational angle of more than 0.03 rad, which meet the requirement recommended by AISC [27] for composite special moment resisting frames.
3. A rational beam-column joint model for the bolted endplate connections was constructed and implemented using general platform ABAQUS. Results showed that analytical models simulate the experimental models well.
4. In both welded and bolted connections, the flexural resistance of the connection increases as the endplate thickness increases.
5. The initial rotational stiffness of the connection increases in both welded and bolted connections due to the increase in the endplate thickness. However, in bolted connections, the sensitivity of this parameter to the endplate thickness is not significant, compared to that of the resistance. In other words, variation of the initial stiffness due to the increase in the endplate thickness is not considerable in bolted connections. Yet, in welded connections, this variation is very remarkable. However, this fact is not true for the flexural resistance of the connections.
6. The endplate thickness does not affect the secondary stiffness of the connection considerably.
7. Generally, the connection rotation in the specific resistance value and the ductility of the connection decrease as the endplate thickness increases in bolted connections.
8. Generally, assuming not failure in the welds and bolts, the rotation (ϕ_{Cd}) increases as the endplate thickness increases in.
9. Welded connections have more rotational stiffness, less ultimate strength, less ultimate rotation and less ductility than that bolted connections do.

10. Bolted connections have more ductility and energy absorption capacity than that welded connections do. Realistic evaluation of the connection ductility, using the finite element method, requires application of the real nonlinear properties of the materials and consideration of the ultimate yielding. This requires a time-consuming analysis. Future studies can focus on development of finite element models in order to conduct more studies on the connection ductility and to find some methods to facilitate the evaluation of the rotational capacity.

6. REFERENCES

- Dunberry, E., LeBlanc, D. and Redwood, R., "Cross-section strength of concrete-filled hss columns at simple beam connections", *Canadian Journal of Civil Engineering*, Vol. 14, No. 3, (1987), 408-417.
- Shakir-Khalil, H. and Mahmoud, M., "Steel beam connections to concrete-filled tubular columns", in Nordic Steel Construction Conference' 95, Malmö. Vol. 19, (1995).
- Alostaz, Y. M. and Schneider, S. P., "Analytical behavior of connections to concrete-filled steel tubes", *Journal of Constructional Steel Research*, Vol. 40, No. 2, (1996), 95-127.
- Alostaz, Y. M. and Schneider, S. P., Connections to concrete-filled steel tubes., University of Illinois at Urbana-Champaign. (1997)
- R., L., "Developments in the use of partial restraint frames in the united states control of semi-rigid behaviour of civil engineering structural connections", *COST Cl. Liege*, (1998), 95-104.
- Swanson, J. A. and Leon, R. T., "Bolted steel connections: Tests on t-stub components", *Journal of Structural Engineering*, Vol. 126, No. 1, (2000), 50-56.
- Swanson, J. A. and Leon, R. T., "Stiffness modeling of bolted t-stub connection components", *Journal of Structural Engineering*, Vol. 127, No. 5, (2001), 498-505.
- HG, P. and AB., d. M., Connecting steel beams to concrete-filled steel columns, in ASCE Structures Congress on Composite Compression Members. San Antonio, (1992) TX. 918-921.
- LL, C., LY, W., GL, H., CF, L. and DH, H., "Experimental study on the design parameters of bidirectional bolted beam-column connections for concrete filled-tube structures", *National Centre for Research on Earthquake Engineering*, (2004).
- Wu, L.-Y., Chung, L.-L., Tsai, S.-F., Shen, T.-J. and Huang, G.-L., "Seismic behavior of bolted beam-to-column connections for concrete filled steel tube", *Journal of Constructional Steel Research*, Vol. 61, No. 10, (2005), 1387-1410.
- Wu, L.-Y., Chung, L.-L., Tsai, S.-F., Lu, C.-F. and Huang, G.-L., "Seismic behavior of bidirectional bolted connections for cft columns and h-beams", *Engineering Structures*, Vol. 29, No. 3, (2007), 395-407.
- Hu, H.-T., Huang, C.-S. and Chen, Z.-L., "Finite element analysis of cft columns subjected to an axial compressive force and bending moment in combination", *Journal of Constructional Steel Research*, Vol. 61, No. 12, (2005), 1692-1712.
- Baig, M. N., Fan, J. and Nie, J., "Strength of concrete filled steel tubular columns", *Tsinghua Science & Technology*, Vol. 11, No. 6, (2006), 657-666.
- Boyd, P. F., Cofer, W. F. and Mclean, D. I., "Seismic performance of steel-encased concrete columns under flexural loading", *ACI Structural Journal*, Vol. 92, No. 3, (1995).
- Roeder, C. W., Cameron, B. and Brown, C. B., "Composite action in concrete filled tubes", *Journal of Structural Engineering*, Vol. 125, No. 5, (1999), 477-484.
- Furlong, R. W., "Strength of steel-encased concrete beam columns", *Journal of the Structural Division, American Society of Civil Engineers*, Vol. 93, (1967), 113.
- Neves, L., Simoes da Silva, L. and Vellasco, P., "Experimental behaviour of end plate i-beam to concrete-filled rectangular hollow section column joints", *International Journal of Applied Mechanics and Engineering*, Vol. 9, No. 1, (2004), 63-80.
- Gioncu, V. and Mazzolani, F., "Ductility of seismic-resistant steel structures", Taylor & Francis, (2003).
- Gaylord, E. H., Gaylord, C. N. and Stallmeyer, J. E., "Design of steel structures", (1992).
- Jaspart, J., "Contributions to recent advances in the field of steel joints-column bases and further configurations for beam-to-column joints and beam splices", *Aggregation thesis. University of Liege*, (1997).
- Girão Coelho, A. M., Bijlaard, F. S. and Simões da Silva, L., "Experimental assessment of the ductility of extended end plate connections", *Engineering Structures*, Vol. 26, No. 9, (2004), 1185-1206.
- Skejic, D., Dujmovic, D. and Androic, B., "Behavior of welded beam-to-column joints subjected to the static load", *Structural Engineering and Mechanics*, Vol. 29, No. 1, (2008), 17-35.
- Simoes da Silva, L., Santiago, A. and Vila Real, P., "Post-limit stiffness and ductility of end-plate beam-to-column steel joints", *Computers & Structures*, Vol. 80, No. 5, (2002), 515-531.
- Kuhlmann, U., Davison, J. and Kattner, M., "Structural systems and rotation capacity", in COST Conference on Control of the semi-rigid behaviour of civil engineering structural connections, Liège, Belgium. (1998), 167-176.
- Bursi, O. and Jaspart, J.-P., "Calibration of a finite element model for isolated bolted end-plate steel connections", *Journal of Constructional Steel Research*, Vol. 44, No. 3, (1997), 225-262.
- Lemonis, M. E. and Gantes, C. J., "Incremental modeling of t-stub connections", *Journal of Mechanics of Materials and Structures*, Vol. 1, No. 7, (2006), 1135-1159.
- Construction, A. I. o. S., "Seismic provisions for structural steel buildings", American Institute of Steel Construction, (2002).

Analytical and Experimental Investigation of I Beam-to-CFT Column Connections under Monotonic Loading

RESEARCH NOTE

G. R. Abdollahzadeh, S. Yapang Gharavi, M. Hoseinali Beigy

Department of civil engineering, Babol University of Technology, Babol, Iran

PAPER INFO

چکیده

Paper history:

Received 29 July 2013

Received in revised form 23 August 2013

Accepted 14 september 2013

Keywords:

Endplate Connection

CFT Column

Moment-rotation Curve

I Beam-to-CFT Column Connection

در این تحقیق مشخصات رفتاری اتصال در اتصالات متشکل از ستون با مقطع قوطی پر شده از بتن (CFT) و تیر I شکل، با انجام آزمایش و مدل‌سازی المان محدود تحت بار یک جهته مورد مطالعه قرار گرفته است. به منظور اعتبارسنجی مدل‌سازی انجام شده با المان محدود، ابتدا یک مدل آزمایشگاهی با مشخصات مشابه ساخته شده و مورد آزمایش قرار گرفت. با بررسی نتایج دو مدل و پس از اطمینان از اعتبار و صحت مدل‌سازی المان محدود، مدل‌های مختلفی در محیط نرم‌افزار ایجاد شدند. پارامترهایی که مورد مطالعه قرار گرفتند شامل ضخامت ورق انتهایی و نوع اتصال می‌باشند. انواع مختلفی از ضخامت ورق انتهایی برای حالات اتصال پیچی و جوشی بررسی شدند. قابل توجه است که انواع اتصال تیر به ستون با ایجاد پیوستگی توسط پیچ‌های عبور کرده از درون مقطع ستون و یا بدون آن‌ها مورد بررسی قرار گرفتند. نتایج حاصله نشان می‌دهند که افزایش ضخامت ورق انتهایی منجر به افزایش مقاومت خمشی اتصال و سختی آن و کاهش دوران در یک مقدار مقاومت خاص می‌گردد.

doi: 10.5829/idosi.ije.2014.27.02b.13

